FACTORS INFLUENCING THREE-PHASE FLOW PARAMETERS IN WAG EXPERIMENTS

Arne Skauge*, Ida Veland**, and Johne Alex Larsen*,
*: Norsk Hydro ASA, N-5020 Bergen, Norway
**: Statoil, Bergen, Norway

Abstract
Immiscible water - alternate-gas (IWAG) experiments are history matched by using the three-phase relative permeability hysteresis option in the ECLIPSE simulator. The paper includes experiments using different core material from two sandstone reservoirs. The IWAG experiments used a water - gas ratio of 1:1, and a slug size of about 0.1 pore volume. The wettability was different for the two core flood cases. The oil recovery by IWAG injection was improved, especially for the intermediate wet core when compared to waterflooding. The paper try to address the question of what three-phase parameters influence the oil recovery, and how these parameters are related. This is an important question with regard to optimizing the IWAG process.

Multivariate analysis has been used to investigate relations between variables like, maximum differential pressure, residual oil saturation, gas and water breakthrough, Land constant (gas trapping), and reduction in three-phase relative permeability compared to two-phase relative permeability. A large number of simulations have been run, by statistically choosing input variables using a most uniform lattice model. A principal component analysis was performed on the results of these simulations. Results of the principal component analysis show that, as an example, the maximum differential pressure is correlated to the water production rate, total production of water, and water three-phase relative permeability. Gas breakthrough was primarily correlated to the gas three-phase relative permeability. The Land constant (gas trapping) had very complex relations in the simulations and the influence on result-groups like oil recovery can not be interpreted from multivariate analysis.

Introduction
The availability of produced hydrocarbon gas has encouraged use of WAG processes in North Sea oil reservoirs[1-5]. The oil recovery by WAG has been attributed to improved sweep, especially recovery of attic oil or cellar oil by exploiting the segregation of gas to the top or accumulation of water towards the bottom. Possible improved microscopic efficiency in three-phase zones of the reservoir may come as an added benefit of the WAG injection.

Experimental studies over many years have shown accelerated oil production and higher recovery in IWAG slug injection as a result of three-phase flow[6-9]. The IWAG process is compared to waterflooding. The objective of these core floods was to generate input rock-type relative permeability data for simulation of an immiscible water-alternating-gas, IWAG. Three-phase effects are also analyzed like; trapped gas, and mobility for secondary processes (ex. water after gas injection). The oil recovery from gas, water, and WAG core displacements are also compared. The oil recovery has been related to the trapped gas saturation[7, 10-11]. The effect of trapped gas is found to be varying with core wettability[12]. Experimental results have shown that both gas and water relative permeability may be reduced during three-phase flow[6-9].

From the experimental observations it became obvious that conventional two-phase relative permeability hysteresis[13,14] was unable to describe the core flow results. Several new ideas directed towards describing three-phase effects were then tested, in order to improve the match and prediction of WAG related experiments[15-18]. These efforts have currently led to the formulation of a phenomenological based WAG hysteresis model[19]. In this paper, we show examples of three-phase parameters found from history match of WAG experiments.

Series of displacements have been carried out on core material from two different sandstone reservoirs. The most significant difference for the two core flood cases is the rock wettability. The immiscible water - alternate-gas (IWAG) experiments are history matched by using the three-phase relative permeability hysteresis option[19] in the ECLIPSE simulator. The paper tries to address the question of what three-phase parameters influence oil recovery, and how the parameters are related.

Multivariate analysis has been used to investigate relation between variables like maximum differential pressure, residual oil saturation, gas and water breakthrough, Land constant (gas trapping), and reduction in three-phase relative permeability compared to two-phase relative permeability. Core flood simulations were performed using input data selected by a most uniform distributed lattice model. A principal component analysis is performed on the results of these simulations.

Experimental

The experimental study includes both primary gas injection and waterflood, and also mobilization after primary processes. Gas injection after the primary waterflood (W1G2) show a mobilization of additional oil, while waterflooding after primary gas (G1W2) gave only very small change in the remaining oil saturation at the end of experiment. Table 1 is showing a summary of the injected volumes, flow rates, initial- and remaining fluid saturations.

The core material was composite sandstone cores from oil reservoirs in North Sea area. The designed composite core A had a diameter of 5.0 cm and a total length of 100 cm. The initial water permeability was 173 mDarcy, while the core average porosity was 28.7 %. The experiments were performed with a temperature of 87.5°C with a 220 bar overburden pressure. Equilibrium oil and gas were recombined reservoir fluids. Injection rate was 4 ml/hr for the continuous gas injections and 12 ml/hr for the continuous water injections. The WAG slug injection was performed at 9.5 ml/h. The slug size was 0.11 PV with water as the first injected fluid. The core B had a diameter of 3.7 cm and a total length of 41 cm. The initial water permeability was 370 mDarcy, while the core average porosity was 21.4 %. Experimental conditions for the core flood were 107°C and 297 bar, using a WAG slug size of 0.1 PV. The first slug injected was gas.

All the continuous displacement experiments have been performed in a vertical situation with gas injected from the top and water injected from the bottom of the core. For the WAG experiments, gravity stable gas cycles were injected from the top of the core, while the core was tilted to a horizontal position during the water injections. Water was then injected from the same end of the core as in the gas injection periods. This procedure is assumed to stabilize the gas front as well as preventing gravity segregation of gas. In the studies of core B water and gas were injected from the same inlet end in all experiments. The tilting of the core during the experiment is assumed to give negligible effects on fluid distribution and for the simulation studies the core is simulated as a vertical oriented core.

Pore size distribution data of the core B from the WAG experiments show a tendency of dual porosity, with one group of pores in the range of $50x10^{-6}$m and the main family of pores at $1 – 10x10^{-6}$m. The large pores may be the cause of early gas breakthrough observed in the gas injection and WAG experiments.

Wettability. Amott tests[20] on WAG cores were used to determine the wettability of the core material. Core A showed a water wet behavior, and only the water phase was imbibed. The wettability index was 0.45 that is a rather high value for reservoir cores. The core B imbibed both water and oil I_w=0.41, while I_o= 0.12, giving a wettability index of +0.29. The results indicate intermediate / slightly water wet conditions. Another indication of the different properties of these cores is the endpoint relative permeability for water floods. The core B had a k_{rw} of 0.45, while the core A show a more water wet behavior with low $k_{rw}(S_{or})$ of 0.08, see Table 1. These results confirm the trend in the wettability measurements.

Core flow results

Core A. Slug injection of gas and water (WAG) gave a remaining oil saturation of 0.24 PV, similar to the oil mobilization by gas injection after waterflood (G2), Table 1. The waterflood results show a low endpoint water relative permeability and little oil production after water breakthrough. Both these observations are indicating a rather water wet core and / or a large capillary end-effect. A large capillary end-effect in the experiment will lower the endpoint water relative permeability and gives a too high remaining oil saturation. The true endpoints have to be estimated from in-situ saturation distribution or from centrifuge data. Gas injection after waterflood shows a reduced gas mobility compared to primary gas injection. Relative permeability hysteresis for gas and water phases are also calculated from the experiments.

Core B. A rather surprising result was the higher oil recovery by water flooding than by gas injection, see Table 1. The gas was as mentioned before injected gravity stable from the top of the core, and a possible explanation for the higher Sor may be the tendency to dual porosity in the core material, or the good recovery by water at intermediate wet condition. A large increase in oil recovery was observed during the secondary

processes compared to the primary recoveries, Table 1. This is also confirmed by the very high oil recovery from WAG compared to primary water or gas injection. In the WAG experiment, gas breakthrough was in the first water cycle after 0.1 PV gas injection.

Three-phase model for relative permeability hysteresis

The major problem in evaluation of three-phase flow and IWAG behavior is the limited experimental information and uncertainties regarding: rate effects on pore-level displacements, capillary end-effect, capillary pressure saturation function (hysteresis), derivation of relative permeability saturation functions, wettability and spreading conditions. However, based on several three-phase flow and WAG experiments, the following key factors seem important for oil recovery and flow behavior[6-9]:

- trapping of gas
- reduced gas mobility in presence of mobile water (compared to two-phase flow)
- reduced water mobility in preference of mobile gas (compared to two-phase flow)
- lowering of residual oil saturation in three-phase flow (oil-spreading behavior).

Details of the three-phase relative permeability hysteresis models can be found in the reference 19 and a discussion of relevant pore-level fluid flow mechanisms is given in reference 21. The relative permeability model[19] has been designed for IWAG processes and involves:

- hysteresis in gas relative permeability
- hysteresis in water relative permeability
- modification of the residual oil saturation in the Stone 1 model.
- coupling of residual oil saturation to trapped gas

Hysteresis in Gas Relative Permeability. The gas phase is found to exhibit strong hysteresis i.e. process dependency. In two-phase water-gas flow in water-wet systems, drainage and imbibition gas relative permeabilities are unequal due to different amount of flowing fraction of the gas saturation. For consolidated porous media the drainage-imbibition hysteresis is mainly caused by the trapping of gas during the imbibition process. The trapping process is usually adequate described by the Land relation[22] for both two-phase and three-phase flow[11]. The Land relation has been used to calculate trapped gas saturation[13,14] and generate imbibition scanning curves. The imbibition scanning curves are assumed to be reversible back to the original hysteresis inflection point for two-phase flow.

The mobility during secondary drainage, calculated by two-phase hysteresis models, is inconsistent with experimental observations, whereas an example gas injection after waterflooding generally has considerably lower gas relative permeability then primary gas injection[8-10]. The three-phase gas relative permeability hysteresis model allows reduced mobility of gas in three-phase situations. Gas trapping is still according to the two-phase hysteresis method of Carlson (Land[21] type relation).

The three-phase oil relative permeability is generated by a modified Stone 1 method[23] The residual oil saturation will be coupled to the trapped gas saturation. This enables the possibility of lower residual oil saturation in three-phase dominated zones and to describe residual oil saturation as function of trapped gas as experimentally observed[6,19]. We have earlier suggested a practical way of redefining the zero oil isoperm in reservoir simulations[15], but the functional dependence of trapped gas is a simpler and less data requiring approach. The oil relative permeability will not follow isoperms but be a part of a new Stone 1 surface for each trapped gas saturation. Thus, oil relative permeability is not fully described by the saturation of two of the phases, but will also be a function of the saturation history or more direct the trapped gas saturation. If a zero oil isoperm is not specified, the smallest of S_{org} and S_{orw} is used as the residual oil saturation (S_{om}) in the Stone I algorithm. This can lead to extreme sensitivity of the saturation value for either S_{orw} or S_{org} on oil recovery since the Stone I algorithm uses the smallest of S_{orw} and S_{org} for calculations of residual oil in three-phase flow. This sensitivity can be observed even though oil relative permeability is set in the order of 10^{-5} for low oil saturations. S_{om} can be replaced if preferred by a table defined zero isoperm named “SOMWAT” in ECLIPSE.

Water three-phase relative permeability model[19] has the flexibility of defining different water relative permeability for two-phase and three-phase situation, and include an interpolation regime for transitions

between two-phase and three phase zones. The hysteresis in water relative permeability is often regarded as negligible in two-phase water-wet systems, but found to increase as the wettability changes towards more weakly water-wet / intermediate- wet[24,25]. However, the three-phase flow hysteresis effect is found to be significant for both water-wet and more intermediate-wet porous media[8]. The limited empirical information available, indicates a dependence of water relative permeability on the historic maximum gas saturation obtained in a hysteresis loop[19]. The saturation function dependency is similar to the treatment of gas hysteresis. However, the calculation of scanning curves does not have any Land relation equivalent.

The WAGHYSTR option as implemented in the ECLIPSE simulator needs the specification of the two-phase (water-oil) water relative permeability curve for increasing water saturation (W1), and a water relative permeability curve (water-oil-gas) for increasing water saturation starting at a maximum attainable gas saturation (W2, W3) Drainage and imbibition scanning curves are interpolated from these two curves after an a priori defined scheme[19].

Simulation of core floods

The different parameters in the WAGHYSTR model must be set by matching the simulator to the experimental pressure and production profiles. The analytical derived relative permeabilities[26] (Figure 1-3) have been used as a first input for history matching the WAG experiment on core A. Analytical relative permeabilitites may by significant effected by the neglect of capillary pressure in the calculation. Further, relative permeabilities may only be determined in narrow saturation intervals for unsteady-state flooding experiments. A first estimate of the reduction coefficient for the gas relative permeability hysteresis is found from the difference between k_{rg}@G1 and k_{rg}@G2 (gas relative permeability for primary gas injection and secondary gas injection, respectively). The analytical gas relative permeabilities (see Figure 1) indicate a reduction coefficient of 0.8.

The high remaining oil saturation after WAG indicates a high residual oil in a three-phase situation and a possible small difference between two-phase residual oil and three-phase residual oil. Since the oil recovery after G2 is only about 0.03 PV lower than for W1, little effect of trapped gas on residual oil is expected. The oil saturation after secondary waterflood, W2 is surprisingly about 0.07 PV lower than G2. Possible explanation could be strong end-effect after G1, which is produced during sec. waterflood. Due to the little change in residual oil saturation, it was decided to run simulations with either only table defined Sor or only trapped gas dependent S_{or}. WAGHYSTR input values for trapped gas saturation are estimated from the Land relation, and the Land constant is fixed and equal to 2.25 for all the simulations. The trapped gas saturation after both W2 and W3 correspond to the same value of the Land constant.

Simulation of the WAG experiment with residual oil dependent on trapped gas. Two different approaches will be presented which all are equal in the case of flow description for gas and water, but with either the table defined or trapped gas dependent residual oil saturation. Capillary pressure is neglected in all of the WAG simulations.

A match is obtained for the WAG experiment by setting residual oil to water; S_{orw} = 0.3, residual oil to gas S_{org} = 0.3 and S_{om} dependency of trapped gas of 0.3. In the literature the residual oil reduction factor has been suggested to be between 0.3 and 1[1,4,13,14]. Simulation results are compared with experimental results in Figure 4-6. The final relative permeabilities are also compared to the analytical relative permeabilities in Figure 1-3.

Water relative permeability, core A. The experimental results can be reproduced by numerical simulation using Corey curves for water relative permeability. The Corey exponent for the water relative permeability is equal for both the 2-phase curve and the 3-phase curve; Nw = 4, but the 3-phase curve has a reduced endpoint of factor 2 compared to the 2-phase curve. The history matched water relative permeability curves are in agreement with the analytical derived water relative permeabilities as seen in Figure 2. Only a minor difference in water relative permeability for high water saturations can be seen for the 2-phase case. The analytical 3-phase water relative permeability curve (W3) shows an unusual shape, however, the water relative permeability curve for G2 indicates that a reduction in water mobility occurs in presence of gas.

Gas Relative permeability, core A. The history matched gas relative permeability is similar to the analytical derived in the case of G1, Figure 1. We refer to reference 19 for the procedure for calculating three-phase gas relative permeability from the (G2) experiment. The gas relative permeability is reduced as water saturation increase above connate water. The best match to gas breakthrough and pressure profile is obtained with the reduction coefficient of 0.5. Although, the three-phase reduction of gas relative permeability may seem little, it has a significant effect on production and pressure profiles.

Oil relative permeability, core A. Two different oil relative permeability curves must be given as input to the STONE I algorithm. The two curves should represent an oil-water system and an oil-gas-irreducible water system that correspond to W1 and G1 in the experimental study, respectively. From Figure 3, it can be seen that the analytical derived k_{row} and k_{rog} show little difference. The history matched oil relative permeabilities are similar to the analytical derived curves, however, k_{row} is slightly above the analytical values and krog slightly below the analytical calculated relative permeabilities.

It was not possible to obtain a Corey-expression for the krog-curve that could match the experimental production and pressure profiles. Production and pressure profiles showed strong dependence on S_{org}. Since the three-phase residual oil saturation is taken as the lowest of S_{orw} or S_{org} and this value is used in equation 2 when SOMWAT has been neglected, strong sensitivity is expected. However, the value of S_{org} may be wrong estimated since it also has sensitivity to three-phase flow. Therefore, the $S_{org} = 0.30$ in the simulations is assumed to be too high, although a perfect match to experimental data is achieved. It is recommended to use SOMWAT-table for calculation of three-phase residual oil. Furthermore, the experimental results did not indicate any effect of reduced residual oil saturation in presence of trapped gas.

The obtained three-phase model for oil, using the modified residual oil in presence of trapped gas, did not match the experimental results from the two continuous injection series, G1W2 and W1G2. In case of W2 the oil recovery was too high and in case of G2 the oil recovery was too low.

It was found that a capillary end-effect must be included in order to match the W1G2 and G1W2 experiment with the same relative permeability description as for the WAG experiments, Figures 7-9. The capillary end-effect was implemented by specifying capillary pressure for water-oil and oil-gas and setting both capillary pressures equal to zero in the well blocks. We will come back to the effect of capillarity for displacements and slug injection in the section on principal component analysis. The simulations match the displacements well, except for the sharp break in oil production during waterflooding in both W1 and W2, Fig. 7-8. The simulations match the core flood gas and water production, as shown in Figure 9. Unsteady state floods like ex. G1W2 in strongly influenced by capillary pressure, while slug injection seems independent of capillarity. This results is a more unique set of matching parameters for the WAG experiment and the history match of the WAG experiment on core A is defined by a Land constant of 2.25, a reduction exponent of 0.5, and no influence of trapped gas on residual oil saturation.

WAG experiment core B. The secondary processes show a strong effect on oil recovery and the WAG experiments support this trend as oil recovery is 92 per cent of oil in place, see Table 1. The simulations had to apply a functional dependency between the residual oil and trapped gas saturation. The trapped gas factor was set equal to 1, which means that trapped gas is substituting residual oil, and the sum of residual hydrocarbon phases stays almost constant. The gas trapping was defined from the sec. water injection, W2 and gave a Land constant of 3.4, also the gas relative permeability was more effected by three-phase flow than in the case of core A. The water relative permeability was reduced by a factor of 10 in three-phase flow (W2) compared to primary water flood (W1), Table 1. Figure 10 shows, simulation of produced phases by using the three-phase hysteresis model. The reduction factor for gas was 4, Land constant equal to 3, and a 10-fold reduction in three-phase water relative permeability.

Analysis of WAG simulation model

The three-phase flow description in the simulation model is based on an empirical database of flow phenomena. The relative permeabilities are thereby not completely free to take any possible values according to, for example, a least-square fit. In fact, they have to incorporate a certain hysteresis logic and saturation dependency. This phenomenological flow description is different from a parameter estimation scheme by the incorporated physical constraints which limits the possible solutions in a complex model to physical feasible

values. The problem of obtaining a global solution to the three-phase saturation oscillation problem is thereby limited by the incorporation of empirical information from a larger database of three-phase flow phenomena.

In the three-phase flow description the parameters are related to specific physical observations on the macroscopic scale. The Land constant, as an example, controls the gas trapping when the gas saturation is decreasing. Furthermore, three-phase reduction factors for gas and water control the ability of gas and water to flow in the three-phase regions. In WAG core-flow experiments cooperative effects coexist and give the final product in terms of saturation profiles, pressure profiles and production profiles. It is important to understand the correlation between macroscopic parameters and the experimental results "observables" in order to extrapolate three-phase behavior from the history matched simulation model at the laboratory scale to a WAG simulation model at the reservoir scale. A novel application based on principal component analysis (PCA) method that gives additional information about the WAG simulation model is presented in this section.

Principal Component Analysis[27]

An experimentally observation is in this paper abbreviated to *an observable* and reflects output data for either an experimentally system or a simulation model. Two observables are said to correlate when the two observables respond in exactly the same way to an external action. The correlation is therefore also connected to the external action itself, different external settings may cause different correlations among observables or some correlations can exist for all external settings. Bivariate correlations may not give a complete interpretation of the multivariate problem.

What is the benefit of using a PCA methodology on a history matched simulation model ?

- the history matching process or parameter estimation scheme will normally not reveal correlation between the parameters and the physical observables
- PCA reveals multivariate correlations[1]*, interaction of phenomena and multi-dimensional structures
- improve physical interpretation of phenomenological hysteresis logic
- implicit verification of simulation model

The multivariate responses are based on several simulations where the simulation model parameters are varied and predicted results from the simulation model are collected for each set of parameters. The choice of result parameters is not arbitrary and should only correspond to measurable quantities. Some core flood results are connected to a specific time like breakthrough of gas and water. Other results could be collected at different time-scale, where for example the oil production from 0 to 40 minutes could be one observable and the oil production from 40 to 60 minutes could be another observable. Some other result parameters are specific related to a physical effect, for example, like the differential pressure peaks that have a minimum pressure value at the gas injection period and a maximum value at the water injection period. Simulation model parameters and result parameters are summarized in Table 2.

The parameter values must also be considered. The "true" values are found from the simulation model that matched the experimental observations, but in order to obtain a multivariate response, these parameters have to be varied within a logical range of values. The range should span the parameter space in such way that all possible responses could be detected. This second assumption may be impossible mainly because **i)** practical issues; only a limited amount of parameter sets is possible to use and **ii)** the multivariate responses may change from one parameter domain to another parameter domain, but such domains are not *a priori* known. There is a minimal possibility that the multivariate responses are effected by the choice of parameter sets if the distance between each parameter set is constant throughout the parameter space. This strategy is known from optimization as "most uniform distributed lattice" [28]

If the correlation between a parameter and an observable is based on the same response from all of the parameter space, the correlation will be denoted as a strong correlation. Accordingly, the same correlation can be seen in all of the principal components. Weaker correlations occurs when a parameter correlate with an observable on one or several subsets of the parameter space. In these occasions a correlation may only occur between a parameter and an observable in one of the principal components. Since the first component

[1]* with correlations is also considered anti-correlations

per definition contains more data information than the second and third principal component, correlations observed from the first principal component will be stronger than correlations observed from the second or third component.

In addition, the observable can be grouped into mutual correlations since some observables can have equal response to parameter variations. For example, the gas breakthrough would probably give the same response as the total gas production in the time interval that includes the breakthrough. The mutual observable correlations give valuable information in a history matching procedure since responses in the same direction would be known. Such quantitative information would otherwise at best be intuitively known from summarizing the experience from the history matching process.

Results from PCA: I) WAG experiment simulated without capillary pressure

The results from using PCA on the simulation model for the WAG core-flow experiment are summarized in Table 3 and commented below. The major items to discuss are; total production, time-dependent production rate, total production and breakthrough times, differential pressure, oil production, and the Land constant.

Total production. The total production of oil, water and gas is restricted by mass-balance given by $S_w+S_o+S_g=1$. From Figure 11, it can be found that that the total production of water and oil is correlated in PC#1 and anti-correlated in PC#2. The total production of gas is always anti-correlated with both oil and water production. Thus, it is possible to increase both the water production and oil production simultaneously, at least for some parameter subsets, but it is impossible to increase both oil and gas production. This is not necessary physical facts , but results from a simulation model that has incorporated empirical information from a large number of three-phase experiments. However, it is believed that an increasing amount of gas accumulation in the core will be beneficial for oil production as long as oil is regarded as the intermediate wetting phase. Accordingly, the total production of oil and gas anti-correlates.

Time-dependent production rate. The response from the phase rate production in the time intervals 0-40 minutes, 40-60 minutes and 60-128 minutes are found to be equal for the gas phase. The oil production rate from 0-40 minutes is not related to the oil production rate from 40-60 and 60 to 128 minutes and the water production rate from 0 to 40 minutes is only weakly related to the water production rate from 40-60 and 60 to 128 minutes. In the time interval 0 to 40 minutes, the production is changed from a mono-phase situation to a three-phase situation. Since oil is the only phase that is produced from start, this phase will be most effected by two- and three-phase production. Both breakthrough of gas and water occur in the 0-40 minutes time interval. Water is injected as the first WAG slug in a two-phase situation, while the second WAG slug is injected in a three-phase situation, that may explain why water production rate at the early period is only weakly connected to the water production rate at later time intervals. Gas is only injected into a three-phase situation and the same response is obtain for all of the time intervals.

Total production and breakthrough time. The total production of gas and water is anti-correlated with the breakthrough time of gas and water, respectively. Total oil production is correlated with total water production and anti-correlated with water breakthrough. A later breakthrough accumulates more of the respective fluids in the core. A high water production level implies that more gas is accumulated in the core and thereby an increase in oil recovery is observed.

Differential pressure. The maximum pressure peak is correlated with the water production rate and both these observables are closely related to the three-phase water mobility reduction factor. The minimum pressure peak is anti-correlated with gas production rate and both these observables are closely related to the three-phase gas mobility reduction factor. In an water-gas injection sequence the differential pressure (dP) increases during injection of water and decreases during injection of gas due to the different viscosity of these fluids. Thus, the oscillation nature of dP versus time in Figure 6 reflects the difference in mobility between water and gas. The transport of the injected fluid depends on the mobility of the fluid in the core, and therefore a smaller buildup of dP during water injection is achieved when there is a high three-phase mobility to water. Similar, a smaller decrease in dP occurs during the gas injection if the three-phase mobility to gas is low.

Oil production. The residual oil saturation to gas is found to be anti-correlated with total oil production as expected. The residual oil saturation to water has limited importance since this is only used in two-phase oil-water systems that is not relevant for the WAG core-flow. Oil production rate in the early period (0-40) is found to correlate with gas three-phase mobility reduction factor, probably due to more stabilized gas-oil front at the lower gas mobility. However, the dependency factor between trapped gas and residual oil gives only a weak correlation with total oil production. This results may seem inconsistent, but is probably caused by the complex parameter interactions for gas trapping.

The Land Constant. The Land constant did not contribute to the three different principal components that have been extracted from the data matrix. Thus, the Land constant is not related to the observables in a structured manner, and the impact of this input parameter is classified as noise by the PCA. Clearly, the Land constant is an important parameter for the WAG core-flow simulation model, which implies that the results are not insensitive for the Land constant. However, the simulation model is based on an assumption that accumulation of gas in the core by a trapping process also decrease the residual oil saturation. The Land constant will therefore influence the production results, not only from its own explicit physical property, but also from an implicit interaction with other parameters. The results from the PCA show that the complex interaction between the Land constant and other parameters does not have specific structures. This observation may have certain implications for an automated parameter estimation scheme, where a global solution of the Land constant could be difficult due to possible local minima related to this parameter. A better approach, which is suitable for parameters with a physical meaning, would be to fix the Land constant based on representative experimental data.

WAG experiment simulated with capillary pressure and capillary end-effects. The capillary end-effect is simulated by including capillary pressure and setting the capillary pressure to zero in the wellblock. Although this is probably not a correct treatment of the end-effect, the literature is lacking information about the capillary end-effect in three-phase systems. Basically, this problem cannot be solved before a clear understanding of three-phase capillary pressure exists. The oversimplified treatment of the end-effect presented in this paper must be put in perspective to the character of the problem.

The production and pressure profiles from WAG core-flow simulations were found to be minor sensitive to the capillary pressure and capillary end-effect. This observation was somewhat surprising, but seems to be related to the three-phase simultaneous production from the WAG core-flow set-up. However, this point should be further investigated.

The results from PCA confirm the above observations since all the major correlations found in the case with no capillary pressure and capillary end-effects included were present also in this second case. However, the general trend was that the correlations was weaker when the capillary pressure is included. This is not surprising since capillary diffusion may have had a minor influence on the in-situ saturation profiles that implies that the relation between the input parameters and the observables may be somewhat weakened.

The injection series G1W2 and W1G2. The main difference between G1W2 and W1G2 core-floods on one hand and the WAG core-flow experiment on the other hand is the number of pore volume that is injected (gas or water) of one fluid before a shift to the other fluid (water or gas). Although, this difference may seem minor in a field perspective, pore-level phenomena can be greatly influenced by the different injection schemes[21].

Opposite to the WAG case, the capillary pressure and in particular the capillary end-effect was found to effect the production and pressure profiles. The capillary pressure was parameterized by a simple approach since the exact shape of the curve was found to be invariant for the predicted results. The two-phase oil-water and gas-oil capillary pressures were therefore multiplied by a given factor in order to see the observable response in the PCA methodology.

The conclusion from PCA is that the predicted results for the G1W2 experiment are rather insensitive for the oil-water capillary pressure and sensitive for the gas-oil capillary pressure. The predicted results for the W1G2 experiments are little influenced by gas-oil capillary pressure and major influenced by the oil-gas capillary pressure. The influence of capillary pressure for both G1W2 and W1G2 is supposed to be related to the capillary end-effect.

Although, there is no physical argument given, it seems that these results confirm the minor influence of capillary pressure on the WAG results as reported previously. The end-effect is observed only to be connected to the two-phase production that is limited in the WAG experiment and is entirely in the primary gas injection (G1) and primary water injection (W1). However, this observation could be a simulation artifact and must be further investigated in additional studies.

In G1W2, the gas-oil capillary pressure is correlated to the breakthrough of gas and anti-correlated with the oil production after G1. Furthermore, the Land constant is correlated to total gas production, however, there is less correlations between the three-phase model an observables in the W1G2 and G1W2 series compared to the WAG case. The explanation for this is probably twofold i) these experiments have less three-phase flow effects than the WAG core-flood and ii) the capillary pressure is far more important for these experiments compared to the WAG case. In W1G2, the oil-water capillary pressure is found to be anti-correlated with oil production after W1 and the water breakthrough.

Conclusions

- the three-phase relative permeability hysteresis model is able to match IWAG core floods
- unsteady state flood like ex. G1W2 was strongly influenced by capillary pressure, while slug injection seemed independent of capillarity
- a novel application of principal component analysis has given additional information about complex three-phase flow simulation models for WAG
- the three-phase flow description could be uniquely determined from a WAG core-flow experiment
- three-phase flow parameters may be difficult to obtain when significant two-phase production occur because of the interaction with capillary pressure and capillary end-effects
- further studies on the capillary end-effect in three-phase core-floods are needed

Acknowledgments

The authors acknowledge Norsk Hydro for permission to publish this work, and Dag Magnus Eriksen for performing simulations as part of the statistical analysis.

References

1. Christensen, J.R., Stenby, E.H., and Skauge, A.: "Review of WAG Field Experience," SPE 39883, presented at the 1998 SPE Mexico Oil and Gas Conference and Exhibition, Villaporosa, Mexico 3-5 March 1998.

2. Hinderaker, L. et al., "IOR Resource Potential of Norwegian North Sea Sandstone Reservoirs Proceedings, 6th European Symposium on Improved Oil Recovery, Stavanger, May 1991, Vol. 2, 957-966.

3. Dalen, V., Instefjord, R., and Kristensen, R.: "A WAG Injection Pilot in the Lower Brent Formation at the Gullfaks Field", 7th European IOR Symposium in Moscow, Russia, October 27-29, 1993.

4. Stenmark, H., and Andfossen, P.O.: " Snorre WAG Pilot - A Case History", 8th European IOR Symposium in Vienna, Austria, May 15-17, 1995. Proceedings Vol. 1, 134-143.

5. Skauge, A., and Berg, E.: "Immiscible WAG Injection in the Fensfjord Formation of the Brage Oil Field," paper 014, proceeding from EAGE, 9th European Symposium on Improved Oil Recovery, The Hague, 20-22 Oct. 1997

6. Olsen, G., Skauge, A., and Stensen, J. .: "Evaluation of the Potential Application of the WAG Process in a North Sea Reservoir," presented at the Sixth European Symposium on Improved Oil Recovery, Stavanger, (May 1991), published in the Revue de l'Institut Francais du Petrole, Jan.-Febr. (1992) 81-93

7. Skauge, A., and Aarra, M.: "Effect of Wettability on the Oil recovery by WAG," Proceedings 7th European Symposium on Improved Oil Recovery, Moscow,(1993), 2, 452-59.

8. Skauge, A., and Larsen, J.A.: "Three-Phase Relative Permeabilities and Trapped Gas Measurements Related to WAG Processes," presented at the 1994 International Symposium of the Society of Core Analysists, Stav., 12-14 Sept., 1994, proceeding paper SCA 9421.
9. Skauge, A., "Summary of Core Flood Results in Connection with WAG Evaluation.", proceedings, the Tenth Wyoming Enhanced Oil Recovery Symposium, University of Wyoming, Sept. 20, 1994, Laramie, Wyoming.
10. Holmgren, C.R., and Morse,R.A.: "Effect of Free Gas Saturation on Oil Recovery by Waterflooding," *Trans*. AIME 192, 135-140 1951.
11. Kyte, J. R., Stanclift, R. J., Stephan, S. C. and Rapoport, L. A.: "Mechanism of Waterflooding in Presence of Free Gas," Pet. *Trans.* AIME 207, 215-221, 1956.
12. Skauge, A.: "Influence of Wettability on Trapped Non-Wetting Phase Saturation in Three-Phase Flow," proceedings Fourth International Symposium on Wettability and it's Effect on Oil Recovery, Montpellier, France, Sept. 1996
13. Killough, J. E.: "Reservoir Simulation with History-Dependent Saturation Functions," Petr. *Trans*. AIME 261, 37-48.
14. Carlson, F.M.: "Simulation of Relative Permeability Hysteresis to the Non-Wetting Phase," SPE 10157, Presented at the 56th Annual SPE Technical Conference and Exhibition, San Antonio, Oct. 5-7, 1981.
15. Skauge, A., and Larsen, J.A.: "New Approach to Model the WAG process.", proceedings, 15th International Energy Agency Collaborative Project on Enhanced Oil Recovery, Workshop and Symposium, Bergen, Norway, 28-31 August, 1994.
16. Skauge, A., and Larsen, J.A.: "Comparing Hysteresis Models for Relative Permeability in WAG Studies," Society of Core Analysts, SCA 9507, Sept. 12-14, 1995
17. Skauge, A.; "Simulation studies of WAG using three-phase relative permeability hysteresis models, paper number 015, proceeding from EAGE, 9th European Symposium on Improved Oil Recovery, The Hague, 20-22 Oct. 1997
18. Christensen, J.R., Stenby, E.H., and Skauge, A.: "Compositional and Relative Permeability Hysteresis Effects on Near Miscible WAG," SPE 39627, proceedings volume 1, 233-49, presented at the SPE/DOE 11th Symposium on Enhanced Oil Recovery, Tulsa, Oklahoma, 20-22 April 1998.
19. Larsen, J.A., and Skauge, A.: "Methodology for Numerical Simulation with Cycle-dependent Relative Permeabilities," Soc. Petr. Enginering Journal, 163- 73, June 1998 (11).
20. Amott, E.: “Observations relating to the Wettability of Porous Rock,” *Petr. Trans*. AIME (1959) Vol 216
21. Larsen, J. A.: "Evaluation of Transport Properties for Immiscible Flow in Porous Media," PhD Thesis, Univ. of Bergen, Nov. 1997.
22. Land, C. S.: "Calculation of Imbibition Relative Permeability for Two- and Three-Phase Flow," Soc. Pet. Eng. J. (June 1968), Pet. Trans. AIME 253, 149-156, 1968.
23. Stone, H.L.: "Probability Model for Estimating Three-Phase Relative Permeability," J.Pet.Tech. (Feb. 1970) 214-218
24. Wei, J. Z., Lile, O. B.: "Influence of Wettability and Saturation Sequence on relative Permeability Hysteresis in Unconsolidated Porous Media," paper SPE 25282, 1992.
25. Braun, E. M. and Holland, R. F.: "Relative Permeability Hysteresis: Laboratory Measurements and a onceptual Model," paper SPE 28615, presented at the SPE 69th annual. Conf., New Orleans (LA), 1995.
26. Virnovskii, G. A.: "Determination of Relative Permeabilities in Three-Phase Flow in a Porous Medium," translated from Izvestiya Akademii Nauk SSSR, Mekhanika Zhidkosti i Gaza, Moscow (Sept.-Oct. 1984) No. 5, 187-89.
27. Lebart, L., Morineau, A., Warwick, K. M.:"Multivariate Descriptive Statistical Analysis," John Wiley & Sons 1984.
28. Chang, J., Ershaghi, I.:"An Improved Microcomputer Approach to Well Test Interpretation. Paper SPE no. 15928, presented at the SPE Eastern Regional Meeting, Columbus, Ohio, Nov. 12-14. 1986.

Table 1. Summary of displacement results.

	Rate	PVinj	Inj.ph. BT	Swi	Sgi	Soi	Swf	Sgf	Sof	Sgi	Sgt	Kri
Core A	(cc/hr)	(pv)	BT, (pv)	%pv								
First gas inj., G1	4	2,5	0,32	27	0	73	27	39,6	33,4			0,22
Sec. waterflood,W2	12	1,35	0,2	27	39,6	33,4	49	20,8	30,2	39,6	20,8	0,03
First waterflood,W1	12	1,4		26,3	0	73,7	67,6	0	32,4			0,08
Sec. gas inj., G2	4	3,1	0,18	67,6	0	32,4	47,4	29,6	23			0,03
Sec. gas inj. Cont.,G2	4.-100	1,2		47,4	29,6	23	41,3	36,1	22,6			0,09
Tert. Waterflood,W3	12	1,1		41,3	36,1	22,6	59,6	17,9	22,5	36,1	17,9	0,03
WAG	9,5	2,5	0,38	71,8	0	28,2	53,8	21,3	24,9			
Waterflood after WAG		2,1		53,8	21,3	24,9	60,4	15,1	24,5		15,1	0,03
Core B												
First gas inj., G1	6	2,4		36	0	64	36	29	35			0,27
Sec. waterflood,W2	6	2,1		36	29	35	70	14	16	29	14	0,05
First waterflood,W1	6	2,5		37	0	63	72	0	28			0,45
Sec. gas inj., G2	6	2,3		72	0	28	46	36	18			0,08
WAG1	6	1,5	0,16	34	0	66	74	21	5		21	
WAG2 (repeated exp.)	6	2,1		43	0	57	75	21	4		21	

Table 2. Observables in PCA

Observables	Description
Gas_BT	gas breakthrough
Wat_BT	water breakthrough
Tot_oil	total oil production
Tot_gas	total gas production
Tot_wat	total water production
P_max	average of the maximum differential pressure peaks
P_min	average of the minimum differential pressure peaks
or0-40	average oil production rate in time interval 0 to 40 hours
or40-60	average oil production rate in time interval 40 to 60 hours
or60-128	average oil production rate in time interval 60 to 128 hours
gr0-40	average gas production rate in time interval 0 to 40 hours
gr40-60	average gas production rate in time interval 40 to 60 hours
gr60-128	average gas production rate in time interval 60 to 128 hours
wr0-40	average water production rate in time interval 0 to 40 hours
wr40-60	average water production rate in time interval 40 to 60 hours
wr60-128	average water production rate in time interval 60 to 128 hours

Table 3. Input parameters to simulation model, parameter intervals in PCA and values found from history matching a WAG core-flow experiment.

Parameter	Description	Min. Value	max. value	history match
LAND	Land constant	1.5	4	2.25
RED.GAS	Reduction of krg from 2-Phase to 3-Phase	0	5	0.5
RED.WAT	Reduction of krw from 2-Phase to 3-Phase	0.25	1	0.5
SORG	Residual oil saturation to gas	0.05	0.35	0.3
A*(Sgt)	Dependency factor of trapped gas on Sor	0	1	0.5

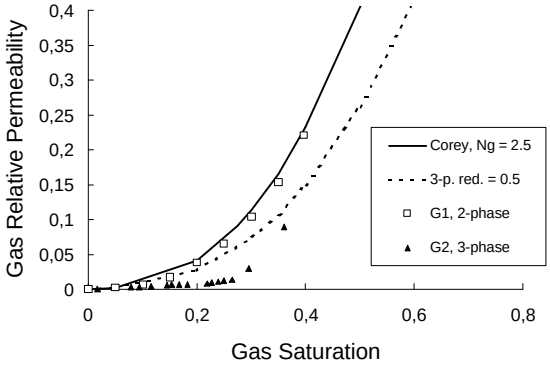

Figure 1. Gas Relative Permeability
(G1,G2 calculated analytical)

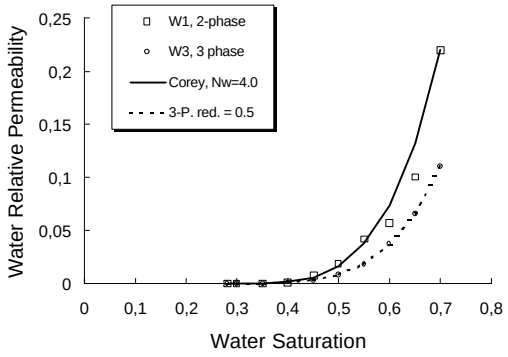

Figure 2. Water Relative Permeability
(W1,W3 calculated analytical)

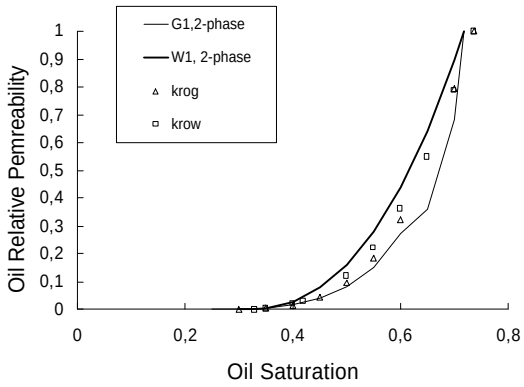

Figure 3. Oil Relative Permeability
(k_{row}, k_{rog} calculated analytical)

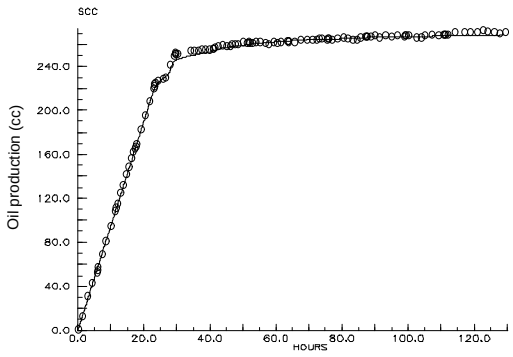

Figure 4. Oil production IWAG, core A,
(lines = simulation)

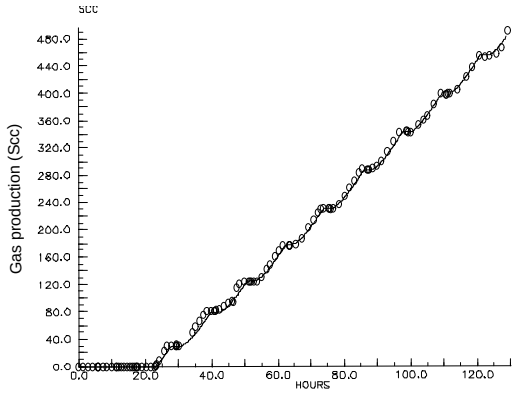

Figure 5. Gas Production, IWAG, core A
(lines = simulation)

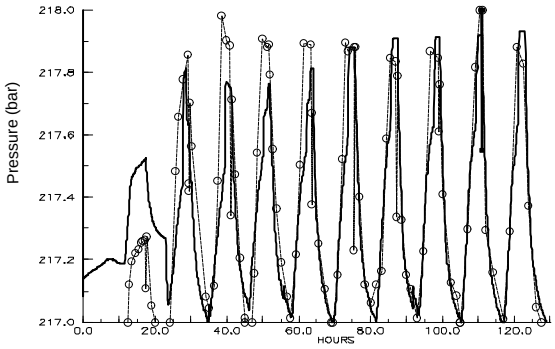

Figure 6. Pressure at inlet, IWAG, core A
(lines = simulation)

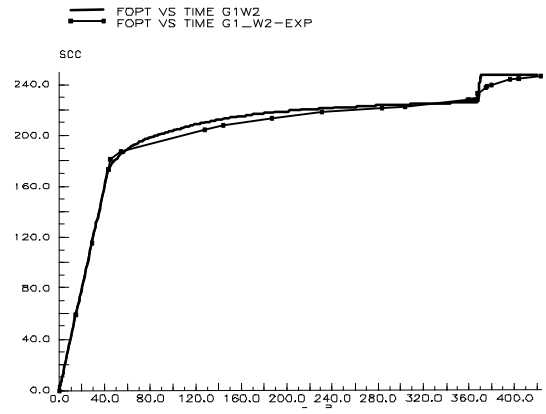

Figure 7. Oil production, G1W2, gas injection followed by water, core A (lines = simulation)

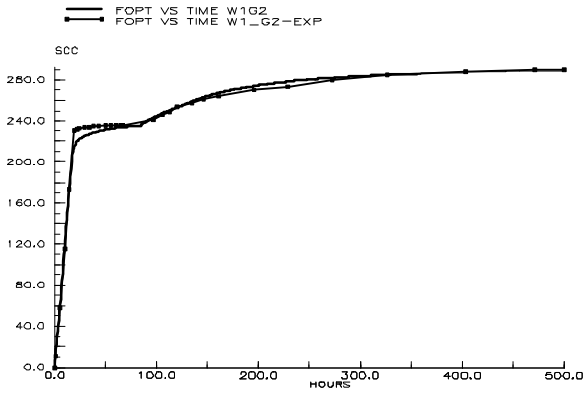

Figure 8. Oil production, W1G2, water injection followed by gas injection, core A, (lines = simulation)

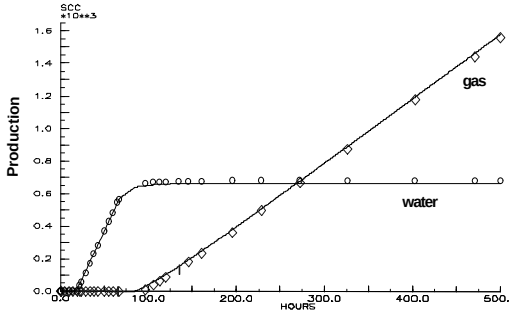

Figure 9. Gas and water production, W1G2, core A (lines = simulation)

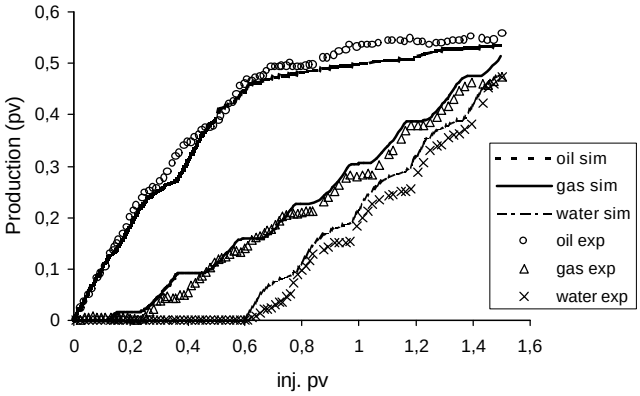

Figure 10. Production from IWAG core B, (lines = simulation)

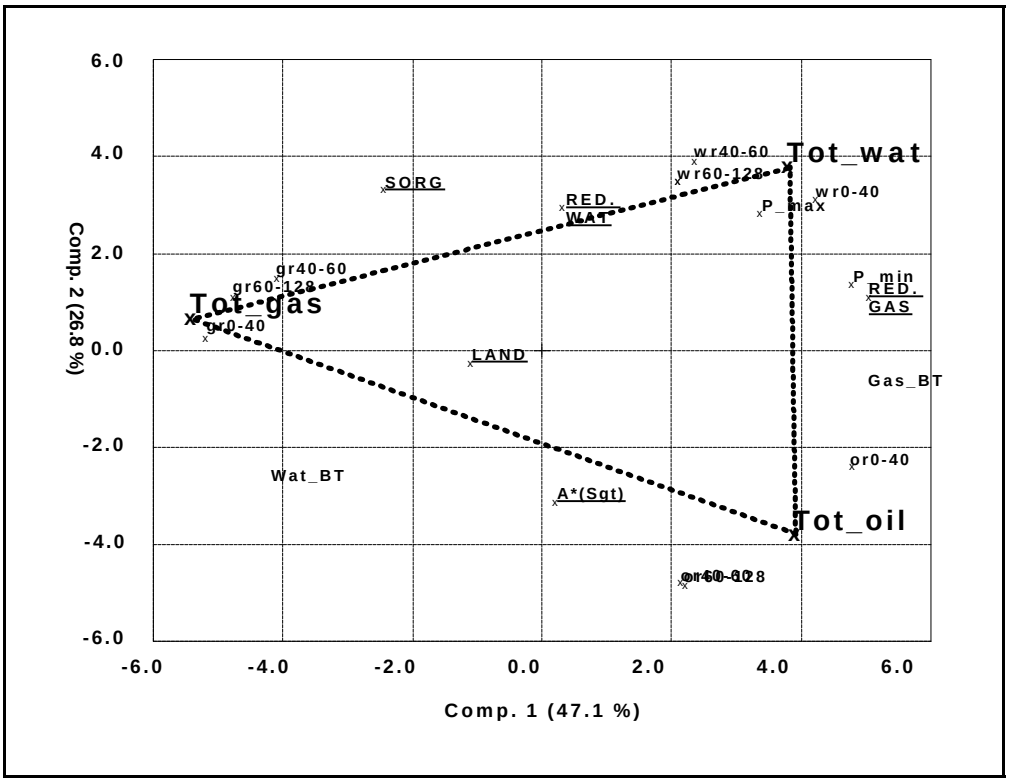

Figure 11. The interaction between total gas, total oil and total water production is clear from the PCA on the simulation model. Total water and total oil production is correlated in the first PC containing most (47.1%) of the original data information, but anti-correlated in the second PC. This indicate that the response on water and oil production is equal in some parameter domains, and opposite in other parameter domains. Total gas production is always nearly anti-correlated with both water and oil production. This plot contains 73.9 % of the original data information and shows all the variables.